Gene regulation underlies environmental adaptation in house mice

Katya L Mack, Mallory A Ballinger, Megan Phifer-Rixey, et al.

Genome Res. published online September 7, 2018
Access the most recent version at doi:10.1101/gr.238998.118

Title: Gene regulation underlies environmental adaptation in house mice

Short title: Gene regulation and adaptation

Katya L. Mack[1], Mallory A. Ballinger[1], Megan Phifer-Rixey[2], Michael W. Nachman[1]

[1]Department of Integrative Biology and Museum of Vertebrate Zoology, University of California, Berkeley, CA 94720, USA
[2]Department of Biology, Monmouth University, West Long Branch, NJ 07764, USA

Corresponding Author:
Michael Nachman
Department of Integrative Biology and Museum of Vertebrate Zoology
3101 Valley Life Sciences Building
University of California, Berkeley 94707
Phone: 510 642-1792
Email: mnachman@berkeley.edu

Keywords: evolution, adaptation, gene regulation

Abstract

Changes in *cis*- regulatory regions are thought to play a major role in the genetic basis of adaptation. However, few studies have linked *cis*- regulatory variation with adaptation in natural populations. Here, using a combination of exome and RNA-seq data, we performed expression quantitative trait locus (eQTL) mapping and allele-specific expression analyses to study the genetic architecture of regulatory variation in wild house mice (*Mus musculus domesticus*) using individuals from 5 populations collected along a latitudinal cline in eastern North America. Mice in this transect showed clinal patterns of variation in several traits, including body mass. Mice were larger in more northern latitudes, in accordance with Bergmann's rule. We identified 17 genes where *cis*-eQTL were clinal outliers and for which expression level was correlated with latitude. Among these clinal outliers, we identified two genes (*Adam17* and *Bcat2*) with *cis*-eQTL that were associated with adaptive body mass variation and for which expression is correlated with body mass both within and between populations. Finally, we performed a gene co-expression network analysis to identify expression modules associated with measures of body size variation in these mice. These findings demonstrate the power of combining gene expression data with scans for selection to identify genes involved in adaptive phenotypic evolution and also provide strong evidence for *cis*- regulatory elements as essential loci of environmental adaptation in natural populations.

Introduction

Understanding the genetic basis of adaptation is a major goal in evolutionary biology. *Cis*-regulatory mutations, which can change the expression of proximal genes, have long been predicted to be important targets for adaptive phenotypic evolution (King and Wilson 1975, Wray 2007, Stern and Orgogozo 2008, Wittkopp and Kalay 2013). One reason for this is that *cis*- regulatory mutations may have fewer deleterious pleiotropic effects than protein-coding changes. While protein- coding mutations may affect protein products across tissues and developmental stages, *cis*- regulatory mutations can affect the expression of genes in spatially and temporally specific ways. In apparent support of this idea, several studies have identified positive selection on non-coding regions (e.g., Jenkins et al. 1995, Crawford et al. 1999, Kohn et al. 2004; Andolfatto 2005; MacDonald and Long 2005; Holloway et al. 2007; Jeong et al. 2008; Torgerson et al. 2009) and an important role for non-coding variation in local adaptation (e.g., Jones et al. 2012, Fraser 2013).

Despite the accumulating evidence that regulatory loci play an important role in adaptive evolution, there are still only a handful of cases where *cis*- regulatory mutations have been linked to ecologically important traits. Among the best examples are adaptive coat color differences in deer mice (Linnen et al. 2013), the ability to digest lactose in humans (Tishkoff et al. 2007), and pelvic reduction in sticklebacks (Chan et al. 2010). Most examples of adaptive gene expression have been identified through candidate gene approaches, which typically favor traits for which components of a pathway are already known and the genetic basis of the trait is relatively simple. However, most traits are influenced by many loci of small to modest effect. Thus, identifying genetic variants

associated with adaptation at complex traits is key to understanding the genetic basis of adaptation.

One avenue for linking adaptive non-coding variation to either molecular or organismal phenotypes is through gene expression. In expression quantitative trait loci (eQTL) mapping, gene expression levels are tested for associations with genetic markers to identify variants that contribute to expression phenotypes. Expression quantitative trait mapping is an effective method for identifying regulatory variants because gene expression is frequently influenced by nearby *cis*-eQTL (Nica and Dermitzakis 2013). *Cis*-eQTL have been successfully detected with small sample sizes (Montgomery and Dermitzakis 2011, Tung et al. 2015) and in wild individuals from natural populations (Tung et al. 2015). Combining eQTL mapping with genomic scans for selection can be a powerful method for identifying the gene targets of adaptive genetic variation (Fraser 2013, Ye et al. 2013) and potentially linking this variation to adaptive organismal phenotypes.

House mice (*Mus musculus domesticus*) provide a useful model for studying the genetic basis of adaptation. House mice are an important biomedical model and have a distribution that mirrors that of human populations (Phifer-Rixey and Nachman 2015). In the eastern United States, house mice show latitudinal variation consistent with local adaptation. Mice collected at northern latitudes are heavier than mice at southern latitudes and their progeny also show differences in a common laboratory environment, indicating that this difference is genetic (Lynch 1992; M Phifer-Rixey, Bi K, KG Ferris, MJ Sheehan, D Lin, KL Mack, SM Keeble, TA Suzuki, JM Good, MW Nachman, *in press*). This observation conforms

to the classic ecogeographic observation known as Bergmann's rule that animals in colder climates have larger mass to reduce heat loss (Bergmann 1847). While Bergmann's rule has been observed in many groups, including humans (Ashton 2000, Ruff 2002, Foster 2013), no study so far has linked this pattern to variation at specific genes. Consistent with energetic adaptation of mice from eastern North America, laboratory strains founded from northern and southern locations also show differences in aspects of blood chemistry, including leptin, glucose, and triglyceride levels (M Phifer-Rixey, K Bi, KG Ferris, MJ Sheehan, D Lin, KL Mack, SM Keeble, TA Suzuki, JM Good, MW Nachman, *in press*).

Recent work with these populations identified hundreds of genes with environmental associations in North American (M Phifer-Rixey, K Bi, KG Ferris, MJ Sheehan, D Lin, KL Mack, SM Keeble, TA Suzuki, JM Good, MW Nachman, *in press*). Here we combine a genomic scan for selection with expression quantitative trait (eQTL) mapping to identify regulatory variants that contribute to gene expression differences and show signals of selection in these populations, identifying two strong candidate genes for adaptive phenotypic variation. To our knowledge, this study represents the first case where genomic scans have been combined with eQTL mapping to identify regulatory variants in natural populations that underlie an adaptive organismal phenotype.

Results

Cis- regulatory variation in wild house mice

To characterize regulatory variation in wild mice, we sequenced liver transcriptomes from 50 mice collected from five populations along a latitudinal transect on the east coast of

North America (Figure 1)(Table S1, File S1). Mice were collected from 29-44°N degrees in latitude. Liver was collected in RNAlater and body mass and length were recorded for each individual. From these individuals, we produced a total of ~1.2 billion RNA-seq reads with an average of 15,473,949 uniquely mapped exonic reads per sample, which were used to quantify gene-wise mRNA abundance (hereafter, gene expression). We also analyzed DNA sequence data generated from exome-capture of the same individuals (M Phifer-Rixey, K Bi, KG Ferris, MJ Sheehan, D Lin, KL Mack, SM Keeble, TA Suzuki, JM Good, MW Nachman, *in press*). Exome and RNA-seq data were used to identify variants segregating in *M. m. domesticus* (see Methods).

We identified *cis*- regulatory variation using two complementary approaches, expression quantitative trait loci (eQTL) mapping and allele-specific expression (ASE). To identify *cis*-eQTLs, we tested for associations between variants within 200-kb of a gene and expression level using a linear mixed model. Variants near a gene are more likely to act in *cis* to affect gene expression. *Cis*-eQTL typically have larger effect sizes than *trans*-eQTL, making then easier to detect in small sample sizes (Montgomery and Dermitzakis 2011). After filtering, a total of 406,999 variants were identified using exome data and tested for associations with expression at 13,080 genes. We identified *cis*-eQTL for 849 of these genes (6.5% of genes surveyed). Reflecting the probe set, the majority of *cis*-eQTL were identified in gene bodies (57%) and introns (18%)(Figure S1).

Allele-specific expression (i.e. differences in expression between parental alleles) can also be used to infer epigenetic or genetic variation acting in *cis* (Cowles et al. 2002). As the two

parental alleles are exposed to the same *trans*- acting environment within an individual, differences in expression at heterozygous sites can be used to infer *cis*- regulatory variation. A total of 28,234 exonic heterozygous sites, corresponding to 6,738 genes, could be tested for ASE. Across all individuals, we found evidence for ASE for 442 genes at a false discovery rate of 5% (6.7% of genes surveyed)(Table S2).

In investigating the power to detect *cis*- regulatory variation, we found that *cis*-eQTL were more likely to be detected when SNP density is higher near and within the gene of interest (Mann-Whitney *U* test, $p<2.2 \times 10^{-16}$)(Figure S2). We were more likely to detect ASE for genes with higher expression and higher SNP density (Mann-Whitney *U* test, $p=3.1 \times 10^{-11}$ and $p<2.2 \times 10^{-16}$, respectively)(Figures S2,S3). While differences in the power to detect ASE and *cis*-eQTL can lead to the identification of different gene sets, we found significant overlap between the gene sets identified with these analyses (hypergeometric test, $p=5 \times 10^{-6}$, Table S2).

Evidence for adaptive regulatory variation

To assess whether the regulatory variation documented above underlies adaptive difference among populations, we studied sequence and gene expression variation along a latitudinal cline (Figure 1a). Clinal patterns of variation can reflect local adaptation as a response to spatially varying selection (Endler 1977). Regulatory variants with clinal frequencies that mediate clinal patterns of gene expression would be strong candidates for adaptive regulatory evolution. To identify such variants, we searched for cases where (1) gene expression is clinal, (2) gene expression is associated with a *cis*-eQTL, and (3) allele

157 frequencies of the *cis*-eQTL vary clinally (Figure 2). While geographic clines may
158 alternatively be explained by isolation by distance, there is no evidence for isolation by
159 distance for these populations (see Supplemental material and methods).
160
161 To identify clinal patterns of gene expression, we tested for correlations between latitude
162 and expression levels in the liver transcriptomes of the 50 wild individuals. We identified
163 1,488 genes for which expression was significantly correlated with latitude (P<0.05), 132
164 of which were associated with a *cis*-eQTL (Figure 2). We also tested for differential
165 expression between the most northern population (New Hampshire/Vermont) and the
166 most southern population (Florida) and identified 458 genes with differential expression
167 between the ends of the cline (Figure S4), 48 of which were associated with a *cis*-eQTL (at
168 q<0.1)(Table S3).
169
170 To connect these patterns to clinal sequence variation, a genome scan using the program
171 Latent Factor Mixed Models (LFMM) was performed to test for correlations between
172 latitude and genetic variation while accounting for population structure (Frichot et al.
173 2013)(see methods). For this study, LFMM has an advantage over other methods because it
174 does not assume a specific demographic model, but still accounts for demographic history
175 by estimating genome-wide co-variance among allele frequencies. We focused on SNPs in
176 the 5% tail of the distribution and considered these clinal outliers (|z-scores|>2)(Figure
177 2a). Blocks of linkage disequilibrium (LD)(Gabriel et al. 2002)(Figure S5) were then
178 inferred to identify co-localization between outlier SNPs and *cis*-eQTL. Of *cis*-eQTL that fell
179 within the same LD block as an outlier, 17 were associated with genes that also show

significant clinal patterns of gene expression (Tables 1,S4)(Figure 2). When comparing the latitudinal extremes, average estimates of F_{st} for these candidate loci were significantly higher than that of the full list of loci (Full list average F_{st}=0.10, candidate average F_{st}=0.34; Permutation test, p=0.0014). Eight of these genes were also significantly differentially expressed between the ends of the cline (Table S5). These 17 genes represent cases where *cis*-eQTL contribute to expression differences between populations and show signals of local adaptation, making them strong candidates for adaptive regulatory variation.

Linking adaptive regulatory variation to specific traits

The liver plays a central role in metabolic processes in the body, and regulatory changes in this tissue may contribute to latitudinal variation in traits related to metabolism. Body mass varies clinally (Figure 1a) and lab born progeny from populations at the ends of the transect also show differences in blood glucose, triglyceride, adiponectin, and leptin levels (Lynch 1992; M Phifer-Rixey, K Bi, KG Ferris, MJ Sheehan, D Lin, KL Mack, SM Keeble, TA Suzuki, JM Good, MW Nachman, *in press*). Four of the 17 candidate genes identified as strong candidates also have mutant phenotypes related to body weight and metabolism. Laboratory mutants for *Cox7c*, and *Hmgb1* are associated with changes in glucose levels (Blake et al. 2017) and mutants for *Adam17* and *Bcat2* are also associated with changes in body mass (She 2007, Wu et al. 2004, Gelling et al. 2008, Blake et al. 2017), glucose (She et al. 2007,24,36), leptin (She et al. 2007, Gelling et al. 2008), and adiponectin levels (Blake et al. 2017, Serino et al. 2007). Another gene identified in this analysis, *Iah1*, transcriptionally regulates genes with important roles in lipid metabolism and triglyceride synthesis and falls under a QTL for fatty liver in mice (Kobayashi et al. 2016, Suzuki et al. 2016).

Adam17 and Bcat2 are candidates for adaptive differences in body mass

While knockout models can provide a link between genotypes and putative phenotypes, these models may not reflect the phenotypic consequences of mutations found in natural populations (Palopoli 1996). Changes in body weight are also among the most common effects of gene knockouts in mice, and may often reflect downstream consequences of other phenotypic changes (Reed et al. 2008, White et al. 2013). While identifying the genetic basis of complex adaptive traits is challenging, gene expression provides an intermediate phenotype that may link sequence variants to organismal traits. To connect adaptive variation in body mass in these populations to genetic variation, we asked whether body mass differences were associated with gene expression differences in the set of candidate genes (Table 1). Since latitude and body mass co-vary in this sample (Figure 1b), we controlled for latitude by regressing it out as a variable. We identified two genes, *A disintegrin and metallopeptidase domain 17*(*Adam17*)(Figure 3A-F) and *branched chain amino acid transaminase 2* (*Bcat2*), for which expression was significantly correlated with body mass, after accounting for latitude as a co-variable (*Adam17*: Pearson's correlation, $p=4.6 \times 10^{-4}$, $R^2=0.22$; *Bcat2*: $p=4.5 \times 10^{-3}$, $R^2=0.17$; see also Table S6, Figure S6). To further account for the possible confounding effects of population structure, we also looked at the correlation between expression level and body mass within each of the five populations. Replicating the pattern seen across populations, *Adam17* expression was negatively associated with body mass in 4 of the 5 populations, and *Bcat2* expression was positively associated with body mass in 4 of the 5 populations (Figure S7,S8). Despite a lack of power for within-population comparisons, the association between *Adam17* expression and body

mass was significant in New Hampshire/Vermont (Pearson's correlation, $p=3.5 \times 10^{-3}$) and the association between *Bcat2* expression and body mass was significant in Pennsylvania (Pearson's correlation, $p=0.03$) and Georgia (Pearson's correlation, $p=1.8 \times 10^{-3}$).

The *cis*-eQTL for *Adam17* and *Bcat2* explain 34% and 29.7% of the variance in expression for theses genes, respectively. Genotypes at these sites were also associated with differences in body mass (Mann-Whitney *U* test, *Bcat2,* TT>CC, $p=0.024$; *Adam17*, CC>TT, $p=0.036$)(Figure S9). Again, co-variation between latitude and body mass can confound relationships between body mass and candidate genes. After regressing latitude from body mass to control for co-variation between these variables, the *Adam17 cis*-eQTL was significantly associated with body mass (Figure 3G)(Cochran-Armitage trend test, $p=0.034$), although the *Bcat2 cis*-eQTL was not (Cochran-Armitage trend test, $p=0.14$). The *Adam17* and *Bcat2 cis*-eQTLs explain an estimated 8.35% and 1.51% of the variation in body mass, respectively. These estimates should be treated as approximations since they may be influenced by (1) unmeasured environmental differences between populations, (2) population structure (even when population structure is accounted for using principle components, as was done here; see Browning and Browning 2011, Dandine-Roulland 2011), (3) imperfect linkage disequilibrium between the surveyed SNPs and causal variants (Wray et al. 2013), and small sample size (Xu 2003). Nonetheless, it is likely that the effect size for the *Adam17 cis*-eQTL is large compared to what is seen in most human GWAS for complex traits (Stranger 2011). Large-effect mutations may be favored in situations where populations are initially far from an optimum (Orr 1998, Dittmar et al. 2016). For example, variation at one gene accounts for a >2 kg weight difference between

Europeans and Inuits (Fumagalli et al. 2015), and a single IGF1 allele in dogs accounts for 15% of variance in dog skeletal size (Sutter et al. 2007). House mice in this transect descended from mice in Western Europe adapted to a Mediterranean climate, and thus likely experienced strong selection pressures in a novel environment, potentially favoring some mutations of large effect.

To investigate regulatory variation at *Adam17* in Western Europe, we retrieved available liver RNA-seq and genomic data from European mice (Harr et al. 2016). We found that the *Adam17 cis*-eQTL is segregating within European populations (Figure S10A) and is significantly associated with liver expression in European individuals (Figure S10B, P=3.2 × 10^{-6}; see Supplemental material and methods). This suggests that adaptation by the large-effect regulatory variation at *Adam17* in the United States is a product of selection on standing genetic variation.

Notably, *Adam17* and *Bcat2* are the two candidate genes from Table 1 with known lab mouse mutants that affect body mass (Wu et al. 2004, She et al. 2007, Gelling et al. 2008, Blake et al. 2017). *Bcat2* encodes a protein that catalyzes the first step of branched-chain amino acid (BCAA) metabolism, which affects metabolism and body mass in humans and rodents (Newgard et al. 2009). *Adam17* encodes a protein that regulates several signaling pathways. Adult *Adam17* heterozygous and null mutants show differences in metabolic phenotypes including body mass, susceptibility to diet induced obesity, and energy homeostasis (Serino et al. 2007, Gelling et al. 2008). ADAM17 and its physiological inhibitor, TIMP3, have also been reported to be involved in the glucose homeostasis and

adipose, hepatic, and vascular inflammation in both genetic and nutritional models of obesity in mice (Fiorentino et al. 2010, Menghini 2012, Matsui 2014). In addition to its association with body mass and metabolism in mice, in humans variation at *ADAM17* has been linked to differences in body weight, BMI, waist circumference, and obesity risk (Junyent et al. 2010) and shows signatures of selection (Pickrell 2009, Parnell et al. 2010, Fumagalli 2011).

One target of ADAM17 activity is the epidermal growth factor receptor (EGFR) signaling pathway (Lee et al. 2003). Phenotypes observed in mice with mutant EGF receptors (including changes in body weight [Blake et al. 2017]) suggest that changes in EGFR signaling as a consequence of deficit ADAM17 activity may contribute to the metabolic phenotypes seen in *Adam17* mutants (Gelling et al. 2008). We tested for an overrepresentation of genes in the EGFR signaling pathway in the set of genes with clinal expression by annotating genes to pathways using the PANTHER database (Thomas et al. 2003). We saw a 1.57-fold enrichment of genes in this pathway compared to a background set of genes expressed in the liver (hypergeometric test, p=0.018). We also find that the gene that encodes the only known physiological inhibitor of *Adam17*, *Timp3* (Le Gall et al. 2010), is differentially expressed between the northern and southern populations (Figure S11, q=0.09) and has expression that is correlated with that of *Adam17* (Figure S11, Pearson's correlation, p=0.02, R^2=0.09). Unlike *Adam17, Timp3* expression is not associated with body mass (Pearson's correlation, p=0.054), although our sample size may not be sufficient to detect an association.

The data above clearly suggest that regulatory variation at *Adam17* and *Bcat2* underlies adaptive differences in body mass, but they do not identify the specific causal mutations. To identify candidate casual mutations, we used annotations from the mouse ENCODE project (Mouse ENCODE Consortium et al. 2012) to search for putative regulatory elements near the *Adam17* and *Bcat2 cis*-eQTLs. The *Adam17 cis*-eQTL is in LD with SNPs through a proximal enhancer and in the *Adam17* promoter, both of which are active in the livers of adult mice. Low-coverage whole genome data show that there are variants segregating within this enhancer in these populations (Figures S12,S13)(whole genome data from [(M Phifer-Rixey, Bi K, KG Ferris, MJ Sheehan, D Lin, KL Mack, SM Keeble, TA Suzuki, JM Good, MW Nachman, *in press*]). Two of the *Adam17* promoter variants are also clinal outliers (Figure S14). The *Bcat2 cis*-eQTL is within an intronic region and is not in LD with annotated regulatory elements that are active in liver tissue.

Expression modules are correlated with body size variation in natural populations of house mice

Next, we used a gene co-expression network approach to identify biologically related gene sets associated with phenotypic variation in these populations. Weighted Gene Co-expression Network Analysis (WGCNA) was used to identify groups of genes with highly correlated expression, called co-expression modules (Langfelder et al. 2008)(see Methods). Expression modules were assigned for male and female mice separately, and then male-female consensus modules were created to identify co-expression patterns shared across sexes.

Co-expression modules were then tested for correlations with measures of body size (Figures S15,S16,S17). Five expression modules in males and five expression modules in females were correlated with trait variation (Figure S18). Trait-associated modules were enriched for a number of Gene Ontology (GO) categories compared to the background set of genes expressed in the liver, including growth factor binding (q=5.3 × 10^{-8}) and lipid metabolic process (q=1.2 × 10^{-2}). None of the male-female consensus modules were significantly correlated with organismal traits, indicating that associations between co-expression modules and traits are sex-specific (Figure S17).

Focusing on the modules with the highest trait correlations (royalblue module in females, corr=0.92, p=2 × 10^{-8} and black module in males, corr=0.8, p=5 × 10^{-8}, for body mass index), we annotated genes with mutant phenotypes collected from Mouse Genome Informatics (MGI)(Blake et al. 2017). Supporting the association between these expression modules and phenotypic variation, we found that many of the genes with high connectivity in these modules have mutant phenotypes related to body size or metabolism (Figure 4). For example, the most connected gene in the female royalblue module is *Nr2c2*. Mutant phenotypes for *Nr2c2* include changes in eating behavior, energy homeostasis, body mass, size, and blood chemistry. Similarly, highly connected genes in the male black module (e.g., *Col3a1, Col1a1, Col1a2, Col5a2, Sparc, Bcam, Fstl1, Igfbp5, Cpe, Cav1, Lamc1, Ltbp3, Krt7*) show mutant phenotypes related to body mass and body size. Four of these genes (*Adamts2*, *Col1a1*, *Col1a2*, *Sparc*) were also identified as hub genes in the module most highly correlated with mouse body weight in another study utilizing an F2 laboratory cross (Ghazalpour et al. 2009).

Finally, we used the co-expression dataset to identify regulatory variation within modules associated with body size. Within the body size associated modules (Figure S18), we associated 189 genes with a *cis*-eQTL, including several highly connected genes in the sex-specific modules with the highest trait correlations (Figure 4). As in the previous analysis, we then searched for genes with a *cis*-eQTL that co-localized with a clinal sequence variant. We identified 15 genes with clinally varying *cis*-eQTL in the body size associated modules (Table S7). We found that gene expression for 4 of these 15 genes was significantly correlated with BMI in one sex (Females: *Ube2q2, p*=0.0002; *3110082I17Rik*, *p*=0.0027; *Cep85*, *p*=0.017; Males: *Pygb p*=0.035). *Cis*-eQTL associated with these genes were not significantly associated with BMI, however, our study is also underpowered for identifying sex-specific associations. The correlation between gene expression and BMI and the presence of clinal *cis*-eQTL make these genes of interest for future study.

Discussion

Identifying loci and genes that underlie adaptive variation within and between populations is a major goal in evolutionary biology. One method used to identify such variants are genomic scans for selection. While many genomic scans attempt to link sequence variants to phenotypes through gene annotations and knockout models, most fail to connect genotypes to phenotypes in natural populations. Here, we used expression data from natural populations of house mice collected along an environmental gradient to link regulatory variation at two genes (*Adam17* and *Bcat2*) with body mass variation. We have linked these genes to body mass variation by 1) associating *cis*-eQTL with the expression of

364 *Adam17* and *Bcat2*, 2) associating the *Adam17* and *Bcat2 cis*-eQTL with body mass
365 variation, and 3) the associating the expression of these two genes with body mass
366 variation. Supporting the association we see between these genes and body mass, mutant
367 alleles for *Adam17* and *Bcat2* in laboratory mice are associated with changes in body mass
368 and metabolism (Wu et al. 2004, She et al. 2007, Serino et al. 2007, Gelling et al. 2008, Blake
369 et al. 2017). Interestingly, these two genes account for a substantial proportion of
370 phenotypic variation in body mass among the mice studied here, with large effect sizes
371 compared to those measured in GWAS for most complex traits. For traits under stabilizing
372 selection within populations (as in virtually all human GWAS) effect sizes are expected to
373 be much smaller than in comparisons between populations experiencing strong divergent
374 selection, as is the case here. The effect size of mutations underlying traits under stabilizing
375 selection within populations is expected to be smaller than the effect sizes of mutations in
376 the early stages of an adaptive walk (Orr 1998, Remington 2015).
377
378 In addition to identifying regulatory variation at specific genes associated with body mass,
379 we also used a systems biology approach to identify co-expression patterns associated with
380 body size variation in wild mice. Gene co-expression networks capture biologically relevant
381 relationships between genes that can be useful for understanding gene functions and
382 interactions. Here we have used this information to characterize co-expression modules
383 that were associated with body size and identified regulatory variation within these co-
384 expressed gene sets that may play a role in body size variation.
385

386 The tendency for body size to increase with latitude (i.e., Bergmann's Rule) has been
387 documented in many species, including humans (Ashton 2000, Ruff 2002, Foster 2013),
388 and reflects an evolved response to differences in temperature (Bergmann 1847). In
389 humans, many candidate genes for metabolic disorders, such as obesity, also show
390 evidence of climatic adaptation (Hancock et al. 2008). Intriguingly, in humans, both
391 *ADAM17* and *BCAT2* have been implicated in metabolic disease (Arribas et al. 2009,
392 Newgard et al. 2009, Junyent et al. 2010, Menghini et al. 2013), and variation at *Adam17*
393 has been identified in genome scans for selection (Pickrell 2009, Parnell et al. 2010,
394 Fumagalli 2011) in addition to its association with body weight and obesity risk (Junyent et
395 al. 2010).
396
397 Finally, this study provides evidence for the role of *cis*- regulatory variation in
398 environmental adaptation in natural populations. While *cis*- regulatory variation has long
399 been hypothesized to play a major role in adaptive phenotypic evolution, connecting
400 regulatory variation with adaptive organismal phenotypes remains tricky. Combining eQTL
401 mapping with genomic scans, as was done here, may be a fruitful approach for identifying
402 adaptive regulatory variation in other natural systems.
403
404 **Methods**
405 *Sampling*
406 Mice used in this study were collected from 5 sampling locations (Table S1, File S1) along a
407 latitudinal gradient in the eastern United States. Mice were sacrificed in the field and
408 measurements (body weight, total body length, tail length) were taken at time of collection.

Body mass index (BMI) was calculated as body weight/length^2 (g/mm^2). Liver tissue was collected in RNAlater and stored at 4^{o}C overnight and then frozen to -80^{o}C until RNA extraction with the Qiagen's RNeasy Mini Kit.

mRNA-sequencing and mapping

For each sample, 100 base-pair paired-end reads were sequenced on the Illumina HiSeq 4000 platform. RNA-seq reads were mapped with TopHat2 (Kim et al. 2013) to personal reference genomes, created by inserting variants into the mouse reference (GRCm38) and masking indels (see Supplemental material and methods). We removed genes with fewer than 500 reads across samples (i.e., an average of 10 reads per sample). Gene expression was then quantile normalized and corrected for hidden factors and known co-variates (individual sex and the first 6 principle components from genotype data to account for population structure) using a Bayesian approach (Stegle et al. 2010, Stegle et al. 2012)(Figure S19,S20).

Exome capture sequencing and identification of clinal outliers

The exome-sequence data was used to identify clinal outliers (M Phifer-Rixey, Bi K, KG Ferris, MJ Sheehan, D Lin, KL Mack, SM Keeble, TA Suzuki, JM Good, MW Nachman, *in press*)(see also Supplemental material and methods). Libraries were enriched for exonic target regions and subsequently 100-bp paired end reads were sequenced on the Illumina HiSeq 2000 platform, resulting in 2 GB of raw sequence data per individual. Forty-one of the 50 individuals for which there is exome- sequence data have matched RNA-seq libraries (see Table S1). Reads were mapped with Bowtie 2 (Langmead and Salzberg 2012) and

allele frequencies were estimated with ANGSD (Korneliussen et al. 2014). LFMM (Frichot et al. 2013) was used to identify covariance between environmental and genetic variation (see Supplemental material and methods).

cis-eQTL discovery

We performed *cis*-eQTL mapping using variant calls from RNA-seq and exome data (see Supplemental material and methods). One limitation of this method is that the genotyping dataset is limited to sites represented by these data (i.e., variant calls are largely limited to exomic regions of the genome). Consequently, many causal sites may not be typed and variants associated with expression may be tagging causal sites in LD. For the exome dataset, depth per site of the targeted exome was ~15 ×. For genes represented in the analysis, on average per individual we had sufficient coverage for ~32% of bases within gene boundaries and ~15% of bases in the 200-kb boundary used as the cut-off for *cis*-eQTL mapping (Table S8).

To identify *cis*-acting eQTLs, we used a linear mixed model applied in the program GEMMA (Zhou et al. 2012) on expression residuals to associate expression with sequence variants (see Supplemental material and methods). A relatedness matrix was computed and included as a covariate. We retained the variant with the lowest *p*-value for each gene and then performed a Bonferroni's correction. Variants with Bonferroni corrected *p*-values of < 0.05 were considered significant.

Weighted gene co-expression analysis

We carried out a weighted gene co-expression network analysis (WGCNA) on expression residuals following WGCNA protocols (Langfelder et al. 2008) to create expression modules. Each module is summarized by a representative eigengene, the first principle component of a given module. Each gene's expression was correlated with the module eigengene as a measure of the gene's centrality to the module, called module membership.

Data access

Illumina sequencing data from this project has been submitted to the NCBI BioProject (https://www.ncbi.nlm.nih.gov/bioproject) under the accession number PRJNA407812. Museum accession numbers for samples used in this study are available in File S1.

Acknowledgements

We thank members of the Nachman lab and three anonymous reviewers for their thoughtful comments and suggestions. This work was supported by an NIH grant (R01 GM074245) to MWN. This work was facilitated by an Extreme Science and Engineering Discovery Environment (XSEDE) allocation to MWN and MPR. XSEDE is supported by National Science Foundation grant number ACI-1548562. KLM is supported by NSF Doctoral Dissertation Improvement Grant (DEB 1601699). MAB was supported by an NSF Graduate Research Fellowship (DGE 1106400).

References

Andolfatto P. 2005. Adaptive evolution of non-coding DNA in Drosophila. *Nature* 437:1149–1152.

Ashton KG, Tracy MC, Queiroz AD. 2000. Is Bergmann's rule valid for mammals? *Am Nat* 156: 390-415.

Arribas J, Esselens C. 2009. ADAM17 as a therapeutic target in multiple diseases. *Curr Pharm Des* 15:2319-2335.

Bergmann C. 1847. Ueber die Verhaltnisse der warmeokonomie der thiere zu ihrer grosse. Gottinger Studien 3: 595–708.

Blake JA, Eppig JT, Kadin JA, Richardson JE, Smith CL, Bult CJ, and the Mouse Genome Database Group. 2017. Mouse Genome Database (MGD)-2017: community knowledge resource for the laboratory mouse. *Nucl Acids Res* 45: D723-D729.

Browning SR, Browning BL. 2011. Population structure can inflate SNP-based heritability estimates. *Am J Hum Genet* 89: 191.

Chan YF, Marks ME, Jones FC, Villarreal G, Shapiro MD, Brady SD, Southwick AM, Absher DM, Grimwood J, Schmutz J, Myers RM. 2010. Adaptive evolution of pelvic reduction in sticklebacks by recurrent deletion of a *Pitx1* enhancer. *Science* 327: 302-305.

Cowles CR, Hirschhorn JN, Altshuler D, Lander ES. 2002 Detection of regulatory variation in mouse genes. *Nature Genet* 32: 432-437.

Crawford DL, Segal JA, Barnett JL. 1999. Evolutionary analysis of TATA-less proximal promoter function. *Mol Biol Evol* 16:194–207.

Dandine-Roulland C, Bellenguez C, Debette S, Amouyel P, Génin E, Perdry H. 2016. Accuracy of heritability estimations in presence of hidden population stratification. *Sci Rep* 6: 26471.

Dittmar EL, Oakley CG, Conner JK, Gould BA, Schemske DW. 2016. Factors influencing the effect size distribution of adaptive substitutions. *Proc R Soc B* 283: 20153065.

Endler JA. *Geographic variation, speciation, and clines* (No. 10). Princeton University Press 1977.

Fiorentino L, Vivanti A, Cavalera M, Marzano V, Ronci M, Fabrizi M, Menini S, Pugliese G, Menghini R, Khokha R, Lauro R. 2010. Increased tumor necrosis factor α–converting enzyme activity induces insulin resistance and hepatosteatosis in mice. *Hepatology* 51: 103-110.

Foster F, Collard M. 2013. A reassessment of Bergmann's rule in modern humans. *PloS ONE* 8: e72269.

Fraser HB. 2013. Gene expression drives local adaptation in humans. *Genome Res* 23: 1089-1096.

Frichot E, Schoville SD, Bouchard G, François O. 2013. Testing for associations between loci and environmental gradients using latent factor mixed models. *Mol Biol Evol* 30: 1687-1699.

Fumagalli M, Moltke I, Grarup N, Racimo F, Bjerregaard P, Jørgensen ME, Korneliussen, TS, Gerbault P, Skotte L, Linneberg A, Christensen C. 2015. Greenlandic Inuit show genetic signatures of diet and climate adaptation. *Science* 349: 1343-1347.

Fumagalli M, Sironi M, Pozzoli U, Ferrer-Admettla A, Pattini L, Nielsen R. 2011. Signatures of environmental genetic adaptation pinpoint pathogens as the main selective pressure through human evolution. *PLoS Genet* 7: e1002355.

Gabriel SB, Schaffner SF, Nguyen H, Moore JM, Roy J, Blumenstiel B, Higgins J, DeFelice M, Lochner A, Faggart M, Liu-Cordero SN. 2002. The structure of haplotype blocks in the human genome. *Science* 296: 2225-2229.

Gelling RW, Yan W, Al-Noori S, Pardini A, Morton GJ, Ogimoto K, Schwartz MW, Dempsey PJ. 2008. Deficiency of TNFα converting enzyme (TACE/ADAM17) causes a lean, hypermetabolic phenotype in mice. *Endocrinology* 149: 6053-6064.

Ghazalpour A, Doss S, Zhang B, Wang S, Plaisier C, Castellanos R, Brozell A, Schadt EE, Drake TA, Lusis AJ, Horvath S. 2006. Integrating genetic and network analysis to characterize genes related to mouse weight. *PLoS Genet* 2: e130.

Hancock AM, Witonsky DB, Gordon AS, Eshel G, Pritchard JK, Coop G, Di Rienzo A. 2008. Adaptations to climate in candidate genes for common metabolic disorders. *PLoS Genet* 4: e32.

Harr B, Karakoc E, Neme R, Teschke M, Pfeifle C, Pezer Ž, Babiker H, Linnenbrink M, Montero I, Scavetta R, Abai MR. 2016. Genomic resources for wild populations of the house mouse, *Mus musculus* and its close relative *Mus spretus. Sci Data* 3: 160075.

Holloway AK, Lawniczak MKN, Mezey JG, Begun DJ, Jones CD. 2007. Adaptive gene expression divergence inferred from population genomics. *PLoS Genet* 3: e187.

Hu Z, Snitkin ES, DeLisi C. 2008. VisANT: an integrative framework for networks in systems biology. *Brief Bioinform* 9: 317–325.

Jeong S, Rebeiz M, Andolfatto P, Werner T, True J, Carroll SB. 2008. The evolution of gene regulation underlies a morphological difference between two *Drosophila* sister species. *Cell* 132: 783–793.

Jenkins DL, Ortori CA, Brookfield JFY. 1995. A test for adaptive change in DNA sequences controlling transcription. *Proc R Soc Lond B* 261: 203-207.

Jones FC, Grabherr MG, Chan YF, Russell P, Mauceli E, Johnson J, Swofford R, Pirun M, Zody, MC, White S, Birney E. 2012. The genomic basis of adaptive evolution in threespine sticklebacks. *Nature* 484: 55-61.

Junyent M, Parnell LD, Lai CQ, Arnett DK, Tsai MY, Kabagambe EK, Straka RJ, Province M, An P, Smith E, Lee YC. 2010. ADAM17_i33708A>G polymorphism interacts with dietary n-6 polyunsaturated fatty acids to modulate obesity risk in the Genetics of Lipid Lowering Drugs and Diet Network study. *Nutr Metab Cardiovasc Dis* 20: 698-705.

Kim D, Pertea G, Trapnell C, Pimentel H, Kelley R, Salzberg SL. 2013. TopHat2: accurate alignment of transcriptomes in the presence of insertions, deletions and gene fusions. *Genome Biol* 14: R36.

King MC, Wilson AC. 1975. Evolution at two levels in humans and chimpanzees. *Science* 108: 107-116.

Kobayashi M, Suzuki M, Ohno T, Tsuzuki K, Taguchi C, Tateishi S, Kawada T, Kim YI, Murai A, Horio F. 2016. Detection of differentially expressed candidate genes for a fatty liver QTL on mouse chromosome 12. *BMC Genet* 17:73.

Kohn MH, Fang S, Wu C-I. 2004. Inference of positive and negative selection on the 5′ regulatory regions of *Drosophila* genes. *Mol Biol Evol* 21:374–383.

Korneliussen TS, Albrechtsen A, Nielsen R. 2014. ANGSD: analysis of next generation sequencing data. *BMC Bioinformatics* 15: 356.

Krzywinski MI, Schein JE, Birol I, Connors J, Gascoyne R, Horsman D, Jones SJ, Marra MA. 2009. Circos: an information aesthetic for comparative genomics. *Genome Res* 19: 1639-1645.

Langfelder P, Horvath S. 2008. WGCNA: an R package for weighted correlation network analysis. *BMC Bioinformatics* 9: 559.

Langmead B, Salzberg SL.Fast gapped-read alignment with Bowtie 2. 2012. *Nat Methods* 9: 357-359.

Lee DC, Sunnarborg SW, Hinkle CL, Myers TJ, Stevenson M, Russell W, Castner BJ, Gerhart, MJ, Paxton RJ, Black RA, Chang A. 2003. TACE/ADAM17 processing of EGFR ligands indicates a role as a physiological convertase. *Ann NY Acad Sci* 995: 22-38.

Le Gall, SM, Maretzky T, Issuree PD, Niu XD, Reiss K, Saftig P, Khokha R, Lundell D, Blobel, CP. 2010. ADAM17 is regulated by a rapid and reversible mechanism that controls access to its catalytic site. *J Cell Sci* 123: 3913-3922.

612 Linnen CR, Poh YP, Peterson BK, Barrett RD, Larson JG, Jensen JD, Hoekstra HE. 2013.
613 Adaptive evolution of multiple traits through multiple mutations at a single
614 gene. *Science* 339: 1312-1316.
615
616 Lynch CB. 1992. Clinal variation in cold adaptation in *Mus domesticus*: verification of
617 predictions from laboratory populations. *Am Nat* 139: 1219-1236.
618
619 MacDonald SJ, Long AD. 2005. Prospects for identifying functional variation across the
620 genome. *Proc Natl Acad Sci USA* 102: 6614–6621.
621
622 Matsui Y, Tomaru U, Miyoshi A, Ito T, Fukaya S, Miyoshi H, Atsumi T, Ishizu A. 2014.
623 Overexpression of TNF-α converting enzyme promotes adipose tissue inflammation and
624 fibrosis induced by high fat diet. *Exp Mol Pathol* 97: 354-358.
625
626 Menghini R, Casagrande V, Menini S, Marino A, Marzano V, Hribal ML, Gentileschi P, Lauro
627 D, Schillaci O, Pugliese G, Sbraccia P. 2012. TIMP3 overexpression in macrophages protects
628 from insulin resistance, adipose inflammation, and nonalcoholic fatty liver disease in
629 mice. *Diabetes* 61: 454-462.
630
631 Menghini R, Menini S, Amoruso R, Fiorentino L, Casagrande V, Marzano V, Tornei F,
632 Bertucci P, Iacobini C, Serino M, Porzio. 2009. Tissue inhibitor of metalloproteinase 3
633 deficiency causes hepatic steatosis and adipose tissue inflammation in mice.
634 *Gastroenterology* 136: 663-672.
635
636 Menghini R, Fiorentino L, Casagrande V, Lauro R, Federici M. 2013. The role of ADAM17 in
637 metabolic inflammation. *Atherosclerosis* 228: 12-17.
638
639 Montgomery SB, Dermitzakis ET. 2011. From expression QTLs to personalized
640 transcriptomics. *Nat Rev Genet* 12: 277-282.
641
642 Newgard CB, An J, Bain JR, Muehlbauer MJ, Stevens RD, Lien LF, Haqq AM, Shah SH, Arlotto,
643 M, Slentz CA, Rochon J. 2009. A branched-chain amino acid-related metabolic signature that
644 differentiates obese and lean humans and contributes to insulin resistance. *Cell Metab* 9:
645 311-326.
646
647 Nica AC, Dermitzakis ET. 2013. Expression quantitative trait loci: present and future. *Phil*
648 *Trans R Soc B* 368: 20120362.
649
650 Orr HA. 1998. The population genetics of adaptation: the distribution of factors fixed
651 during adaptive evolution. *Evolution* 52: 935-949.
652
653 Palopoli MF, NH Patel. 1996. Neo-Darwinian developmental evolution: can we bridge the
654 gap between pattern and process? *Curr Op in Gen and Dev* 6: 502-508.
655
656 Parnell LD, Lee YC, Lai CQ. 2010. Adaptive genetic variation and heart disease risk. *Curr*
657 *Opin Lipidol* 21: 116.

Phifer-Rixey M, Nachman MW. 2015. The Natural History of Model Organisms: Insights into mammalian biology from the wild house mouse *Mus musculus. eLife* 4: e05959.

Pickrell JK, Coop G, Novembre J, Kudaravalli S, Li JZ, Absher D, Srinivasan BS, Barsh, GS, Myers RM, Feldman MW, Pritchard JK. 2009. Signals of recent positive selection in a worldwide sample of human populations. *Genome Res* 19: 826-837.

Reed DR, Lawler MP, Tordoff MG. 2008. Reduced body weight is a common effect of gene knockout in mice. *BMC Genet* 9:4.

Remington, D. L. (2015). Alleles versus mutations: understanding the evolution of genetic architecture requires a molecular perspective on allelic origins. *Evolution* 69:3025-3038.

Ruff C. Variation in human body size and shape. 2002. *Annu Rev Anthropol* 31; 211-232.

Serino M, Menghini R, Fiorentino L, Amoruso R, Mauriello A, Lauro D, Sbraccia P, Hribal, ML, Lauro R, Federici M. 2007. Mice heterozygous for tumor necrosis factor-α converting enzyme are protected from obesity -induced insulin resistance and diabetes. *Diabetes* 56: 2541-2546.

She P, Reid TM, Bronson SK, Vary TC, Hajnal A, Lynch CJ, Hutson M. 2007. Disruption of BCATm in mice leads to increased energy expenditure associated with the activation of a futile protein turnover cycle. *Cell Metab* 6: 181-194.

Mouse ENCODE Consortium et al. 2012. An encyclopedia of mouse DNA elements (Mouse ENCODE). *Genome Biol* 13: 418.

Stegle O, Parts L, Durbin R, Winn J. 2010. A Bayesian framework to account for complex non-genetic factors in gene expression levels greatly increases power in eQTL studies. *PLoS Comput Biol* 6: e1000770.

Stegle O, Parts L, Piipari M, Winn J, Durbin R. 2012. Using probabilistic estimation of expression residuals (PEER) to obtain increased power and interpretability of gene expression analyses. *Nat Protoc* 7: 500-507.

Stern DL, Orgogozo V. 2008. The loci of evolution: how predictable is genetic evolution? *Evolution* 62: 2155-2177.

Stranger BE, Stahl EA, Raj T. 2011. Progress and promise of genome-wide association studies for human complex trait genetics. *Genetics* 187: 367-383.

Sutter NB, Bustamante CD, Chase K, Gray MM, Zhao K, Zhu L, Padhukasahasram B, Karlins E, Davis S, Jones P, Quignon P. 2007. A single IGF1 allele is a major determinant of small size in dogs. *Science* 316: 112-115.

Suzuki M, Kobayashi M, Ohno T, Kanamori S, Tateishi S, Murai A, Horio F. 2016. Genetic dissection of the fatty liver QTL Fl1sa by using congenic mice and identification of candidate genes in the liver and epididymal fat. *BMC Genet* 17: 145.

Thomas PD, Campbell MJ, Kejariwal A, Mi H, Karlak B, Daverman R, Diemer K, Muruganujan A, Narechania A. 2003. PANTHER: a library of protein families and subfamilies indexed by function. *Genome Res* 13: 2129-2141.

Tishkoff SA, Reed FA, Ranciaro A, Voight BF, Babbitt CC, Silverman JS, Powell K, Mortensen, HM, Hirbo JB, Osman M, Ibrahim M. 2007. Convergent adaptation of human lactase persistence in Africa and Europe. *Nature Genet* 39: 31-40.

Torgerson DG, Boyko AR, Hernandez RD, Indap A, Hu X, White TJ, Sninsky JJ, Cargill M, Adams MD, Bustamante CD, et al. 2009. Evolutionary processes acting on candidate cis-regulatory regions in humans inferred from patterns of polymorphism and divergence. *PLoS Genet* 5:e1000592.

Tung J, Zhou X, Alberts SC, Stephens M, Gilad Y. 2015. The genetic architecture of gene expression levels in wild baboons. *eLife* 4: e04729.

White JK, Gerdin AK, Karp NA, Ryder E, Buljan M, Bussell JN, Salisbury J, Clare S, Ingham NJ, Podrini C, Houghton R. 2013. Genome-wide generation and systematic phenotyping of knockout mice reveals new roles for many genes. *Cell* 154: 452-464.

Wittkopp PJ, Kalay G. 2012. *Cis*-regulatory elements: molecular mechanisms and evolutionary processes underlying divergence. *Nat Rev Genet* 13: 59-69.

Wray GA. 2007. The evolutionary significance of *cis*-regulatory mutations. *Nat Rev Genet* 8: 206.

Wray NR, Yang J, Hayes BJ, Price AL, Goddard ME, Visscher PM. 2013. Pitfalls of predicting complex traits from SNPs. *Nat Rev Genet* 14: 507-515.

Wu JY, Kao HJ, Li SC, Stevens R, Hillman S, Millington D, Chen YT. 2004. ENU mutagenesis identifies mice with mitochondrial branched-chain aminotransferase deficiency resembling human maple syrup urine disease. *J Clin Invest* 113: 434-440.

Xu S. 2003. Theoretical basis of the Beavis effect. *Genetics* 165: 2259-2268.

Ye K, Lu J, Raj SM, Gu Z. 2013. Human expression QTLs are enriched in signals of environmental adaptation. *Genome Biol Evol* 5: 1689-1701.

Zhou X, Stephens M. 2012. Genome-wide efficient mixed-model analysis for association studies. *Nature Genet* 44: 821-824.

Figure Legends

Figure 1. A. Sampling locations along the east coast of North America (climate map obtained from NOAA, National Weather Service). B. Consistent with Bergmann's Rule, body mass in mice increases with increasing latitude (Pearson's correlation=0.34, p=0.018)(see Table S9)(See Supplemental material and methods).

Figure 2. Overlap between genomic scans identifies regulatory variants that are candidates for clinal adaptation. A. The LFMM |z-scores| for each SNP vs. chromosome position. SNPs with |z-scores|>2 were considered clinal outliers. B. Manhattan plot of *cis*-eQTL. Shown in red are significant SNPs. C. Manhattan plot of gene starting position vs. the correlation between gene expression and latitude. Points labeled in orange are genes for which expression is significantly correlated with latitude (p<0.05). On the outside are ideograms with the location of genes for which these three signals (A,B,C) overlap. Figure created with Circos (Krzywinski et al. 2009).

Figure 3. *Adam17* is a candidate for adaptive differences in body mass among mice in eastern North America. A. Expression of *Adam17* is correlated with latitude (p=0.032, Pearson's correlation=-0.30). Sex was not a significant predictor of *Adam17* expression. B. A SNP at Chr12:21332631 was identified as a *cis*-eQTL for *Adam17.* C. Allele frequencies of Chr12:21332631 in five populations. D. The LFMM |z-scores| for sites on Chromosome 12 versus position. Points above the red line were considered clinal outliers in this study. The red box represents the peak in which Chr12:21332631 is found. E. Nearby outlier SNPs in LD with Chr12:21332631. Correlations (r^2, %) are given in each block. The z-scores for each site's association with latitude are given in parentheses. F. *Adam17* expression is significantly associated with body mass when controlling for latitude (Pearson's correlation, $p=4.6 \times 10^{-4}$, R^2=0.22). G. Genotype at Chr12:21332631, the *cis*-eQTL for *Adam17*, significantly trends with body size when latitude is controlled for (Cochran-Armitage trend test, p=0.034).

Figure 4. Visualization of the most connected genes in the female "royalblue" (A) and the male "black" with co-expression modules with VisANT (Hu et al. 2008) (B). The royalblue module is associated with BMI ($p=2 \times 10^{-8}$) and body length variation ($p=6 \times 10^{-6}$). The black module is associated with BMI ($p=5 \times 10^{-8}$), body mass (p=0.001), and body length variation ($p=3 \times 10^{-10}$). Blue circles represent genes for which we identified a *cis*-eQTL that explains a component of expression variation. Circles with black borders are genes with mutant phenotypes related to body size or metabolism. Phenotype information was collected from MGI (Blake at al. 2017).

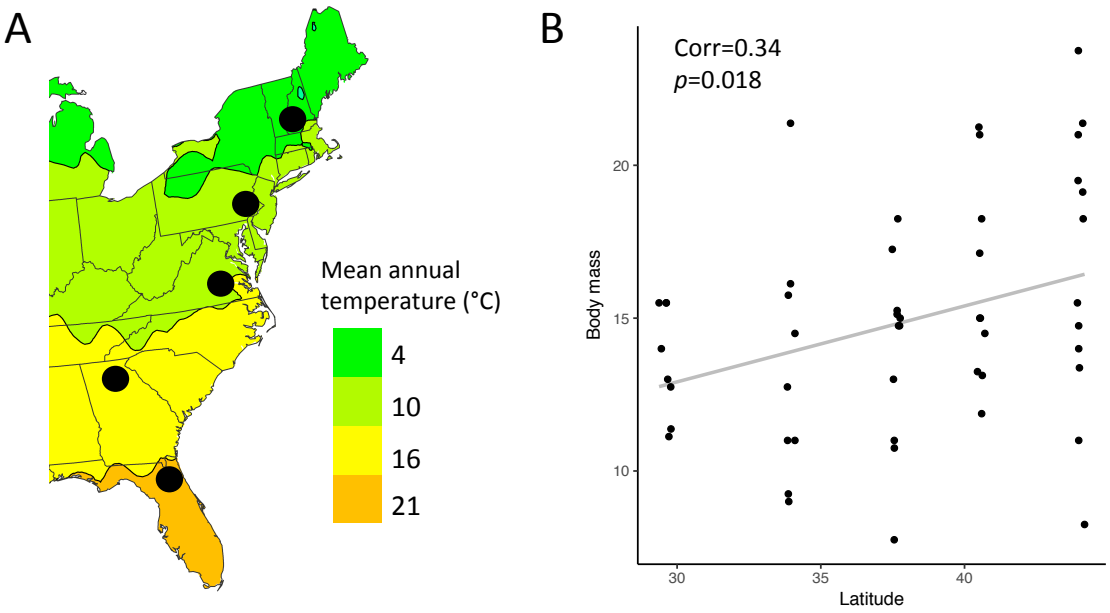

789

790

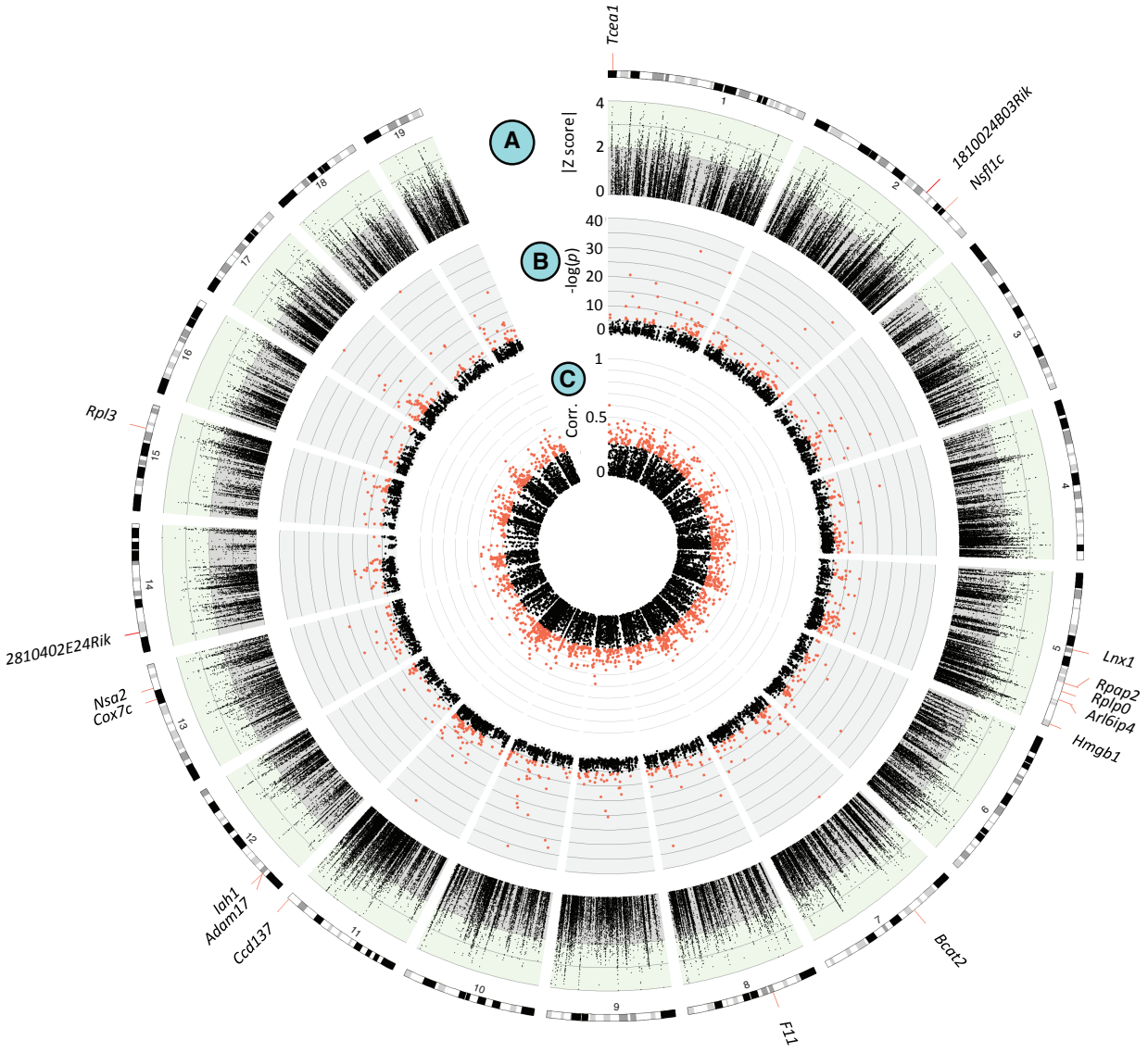

791

792

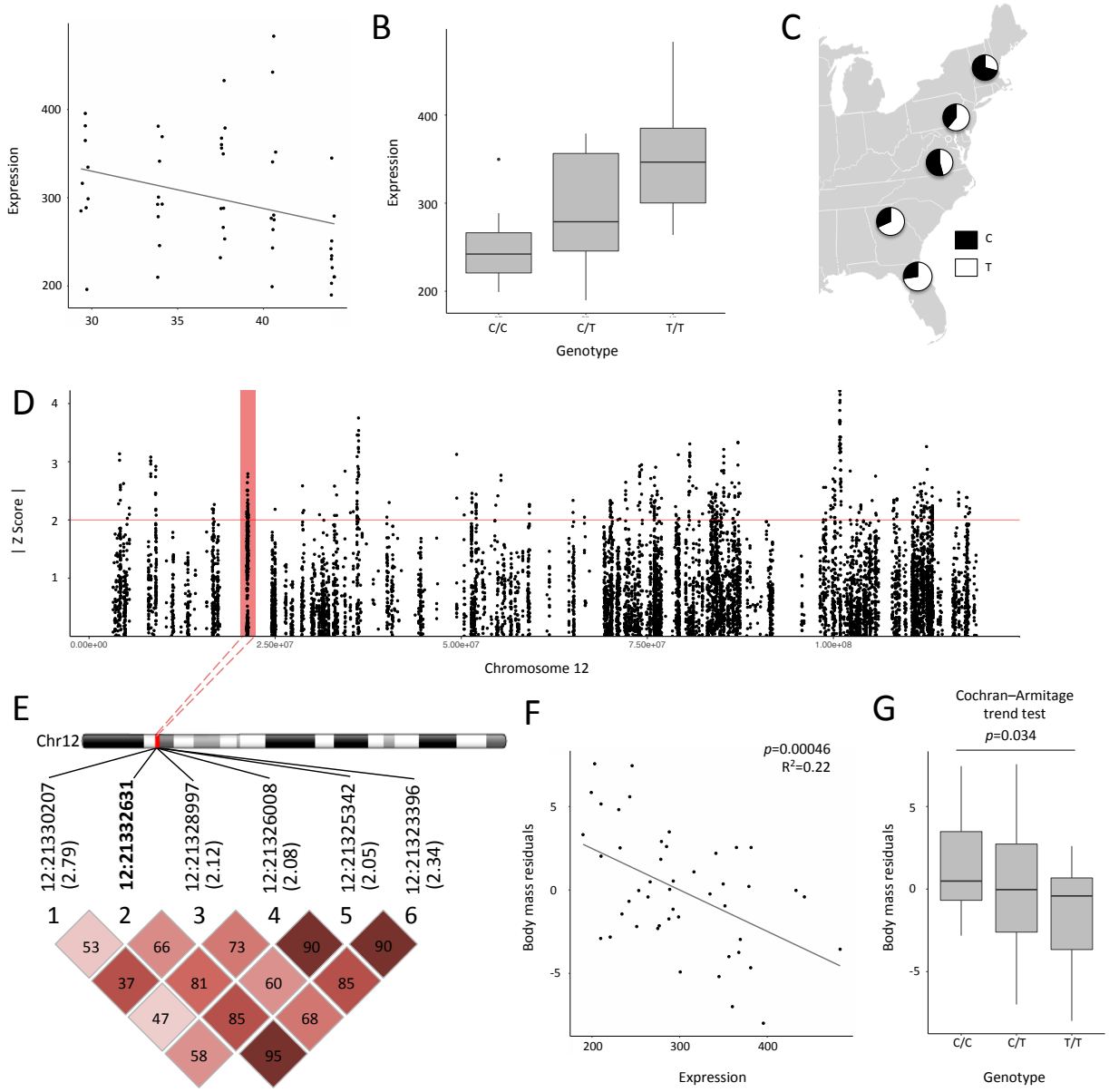

793
794
795

A

Female royalblue module

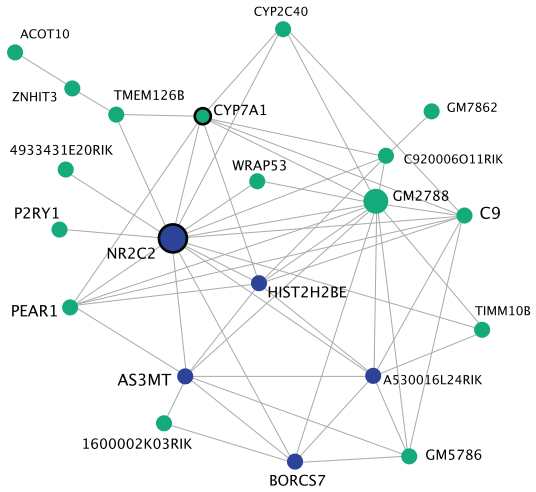

B

Male black module

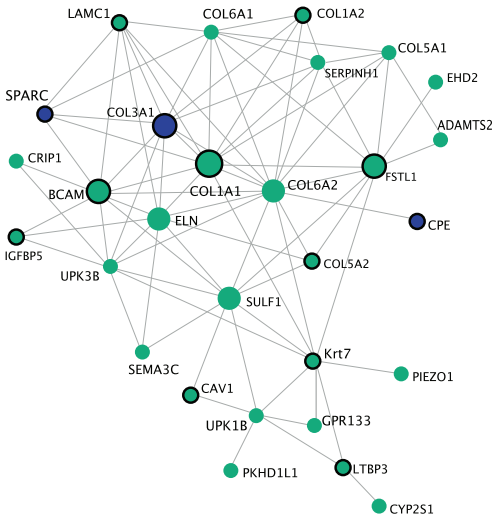

796

Table 1. *cis*-eQTL that co-localize or are within the same LD block as a clinal outlier that also show expression changes correlated with latitude.

Symbol	Correlation with latitude	*p*-value	Phenotypes[1]
Tcea1	0.6	3.66E-06	cardiovascular, embryo, growth/size/body, hematopoietic, homeostasis, limbs/digits/tail, liver/biliary, mortality/aging
Iah1	-0.43	0.0018	cardiovascular, limbs/digits/tail, skeleton
Lnx1	-0.41	0.0035	hematopoietic, immune
2810402E24Rik	0.38	0.0073	
Arl6ip4	0.36	0.0096	
Nsa2	-0.36	0.011	
Rpl3	0.35	0.014	
Bcat2	0.34	0.016	adipose, behavior, growth/size/body, homeostasis, renal/urinary
1810024B03Rik	-0.32	0.023	
Rplp0	0.32	0.023	hematopoietic, immune
Rpap2	-0.32	0.023	
F11	0.31	0.027	hematopoietic, homeostasis, nervous system
Hmgb1	0.31	0.031	endocrine/exocrine, homeostasis, immune, cellular, hematopoietic, mortality/aging, behavior, growth/size/body, mortality/aging, respiratory, vision/eye
Adam17	-0.3	0.032	cardiovascular, cellular, digestive/alimentary, embryo, growth/size/body, hematopoietic, homeostasis, immune, integument, mortality/aging, muscle, nervous system, pigmentation, respiratory, vision/eye
Cox7c	-0.3	0.035	homeostasis, mortality/aging
Ccdc137	0.29	0.041	
Nsfl1c	0.28	0.0496	

[1]Abnormal phenotypes in targeted gene mutants, collected from Mouse Genome Informatics database (MGI)